The Effect of Temperature Variance with Different Surface Shapes on Efficiency of Silicon Thin Film Solar Cell

Khalil Mahmoud ElKhamisy (k.mahmoud@sha.edu.eg)
El-Shorouk Academy: Shorouk Academy https://orcid.org/0000-0002-3423-5356
Hamdy AbdElhamid
Ajman University of Science and Technology College of Engineering
salah Elagooz
El-Shorouk Academy: Shorouk Academy
El-Sayed El-Rabaie
Menoufia University

Research Article

Keywords: Thin film solar cell, Surface grating, Solar cell efficiency, reverse saturation current, temperature effect

Posted Date: September 17th, 2021

DOI: https://doi.org/10.21203/rs.3.rs-799816/v1

The Effect of Temperature Variance with Different Surface Shapes on Efficiency of Silicon Thin Film Solar Cell

Khalil ElKhamisy[1], Hamdy Abdelhamid[2,3], Salah Elagooz[1], and El-Sayed El-Rabaie [4]

[1] Department of Communications and Computers Engineering, The Higher Institute of Engineering , El-Shorouk City 11837, Egypt
[2]Faculty of Engineering and Information Technology, Electrical Engineering Department, Ajman University, Ajman, United Arab Emirates
[3]Center of Nano-Electronics and Devices (CND), Zewail City of Science and Technology, 6th October City, Egypt
[4]Department of Electronics and Communications Faculty of Electronic Engineering, Menoufia University, Egypt

(Corresponding Author: **Khalil ElKhamisy,** mail: k.mahmoud@sha.edu.eg)

Abstract – **In this work, the temperature effects on the PV's electrical and optical parameters of different surface gratings are studied. A 3D simulation is introduced for studying the PV's electrical parameters such as short circuit current, open circuit voltage and efficiency at different levels of temperature with and without surface's gratings. We observed that the efficiency is increased for PV of surface grating by about 4.87% compared to the free grating surface's PV. The efficiency of the PV efficiency is degraded as we increased the temperature above 300K. The solar cell efficiency of gratings free is aggressively degraded compared to the solar cell that includes gratings by about 4.89% at 360K. The electrical parameters such as the open circuit voltage and short circuit current are enhanced compared to the PV of surface grating free. Also, we observed that the triangle grating geometry of dimensions about 10×10 nm produced a higher efficiency compared to the other PV of other grating geometries of same dimensions.**

Keywords **Thin film solar cell, Surface grating, Solar cell efficiency, reverse saturation current, temperature effect.**

1. INTRODUCTION

The technique of directly transforming sunlight into energy using solar cells is known as photovoltaic. It is now a fast expanding and more significant renewable alternative to traditional fossil fuel energy generation. The energy is low cost, renewable and friendly to the community **[1]**.

The thin film solar cells have lowered costs by substituting the bulk substratum for thin film layers rather than bulk. The main problem is to reduce the absorbed energy level to the semiconductor material energy gap using thin film technology. The advantages are different in

thin-film silicone solar cells but they want to achieve moral efficiency and improve production methods. Solar-cell technology of thin film silicone has confronted new crystalline silicon cells with the use of a limited number of active ingredients and low thermal growth although crystalline silicon based solar cells grow rapidly in thin-film **[2-4]**.

Many studies have shown that the efficiency of solar cells decreases as temperature rises due to the recombination process. The electrical properties of a solar cell, such as the density of short-circuit current (Jsc), and open circuit voltage (Voc) are essential parameters used to study the efficiency (η) **[5–11]**. The temperature values of 15 ºC (288 K) to 50 ºC (323 K) and even greater are used to study the solar cells behavior **[12]**.

Many papers have been published in recent years that use gratings of various structures to improve the efficiency of thin-film solar cells **[13]**. In **[14]**, the effects of grating geometry and their dimensions effects on the optical and electrical parameters and hence on the efficiency of thin film solar cells were reported. This research was presented using 3D numerical simulation results produced from the Multiphysics simulator. When a half circle grating was used instead of a solar cell without a grating, the PV efficiency has been increased by 1.27 %. Another research was presented for different surface grating shapes and their effects on the optical, electrical, and efficiency of a thin film solar cell model **[14]**. In the case of triangular grating, the PV efficiency increased by 4.51 %. The absorbance coefficients of the two models increase the photon absorbance by 20% for both types **[15].**

In this paper, we are proposing three different surface gratings' models to study the impact of temperature on the electrical parameters and efficiency. In this work, the study is introduced by using a 3D numerical simulation. Both optical and electrical models are integrated and applied to the thin film solar cell models. The solar cell parameters such as short circuit current, open circuit voltage and efficiency are extracted and analyzed at different temperature levels. The transport models used in this work are semiconductors model (including the drift diffusion and electrostatic modules) besides the electromagnetic module to study the optical behavior.

The rest of this paper is organized as follows: Section 2 solar cell's model and structure are explained. Section 3 transport models used in the study are explained and studied. In Sec. 4, parameters extractions including the impact of the temperature on the device behavior are also introduced and finally the conclusions are presented in Sec. 5.

2. DEVICE STRUCTURE

The importance of introducing surface grating has been studied in **[15]**, the authors achieved significant improvements in term of PV in case of triangle grating by 20% increase on photon absorbance in the modeled solar cell, simulation of dimensions (10×10 nm).

The typical structure of solar cell is shown in Fig. 1a, consists of five stacked layers as, (1) Anode P++ collecting layer at the top, (2) Absorption intrinsic a-Si layer structure,

(3) Cathode N++ collecting layer, (4) Protective ZnO Layer, and (5) the whole layer structure constructed on top of the reflector behind.

Figures 1(a-c) represent the proposed structures of different grating shapes in this work. The new structures are obtained from the typical one, the proposed structures are classified according to the applied shapes of grating as: Fig. 1a of free grating **[16]**, Fig. 1b presents the proposed model of surface grating (5×5 nm) dimensions and the last model, Fig.1c of deep surface gratings (10×10 nm). Please notice, the proposed structures' dimension is shown on respected figure. The dimensions for grating are clearly presented in Fig.1 and the horizontal spacing between the SPPs gold layers is 30 nm. The model parameters used along this work are presented in Table. 1.

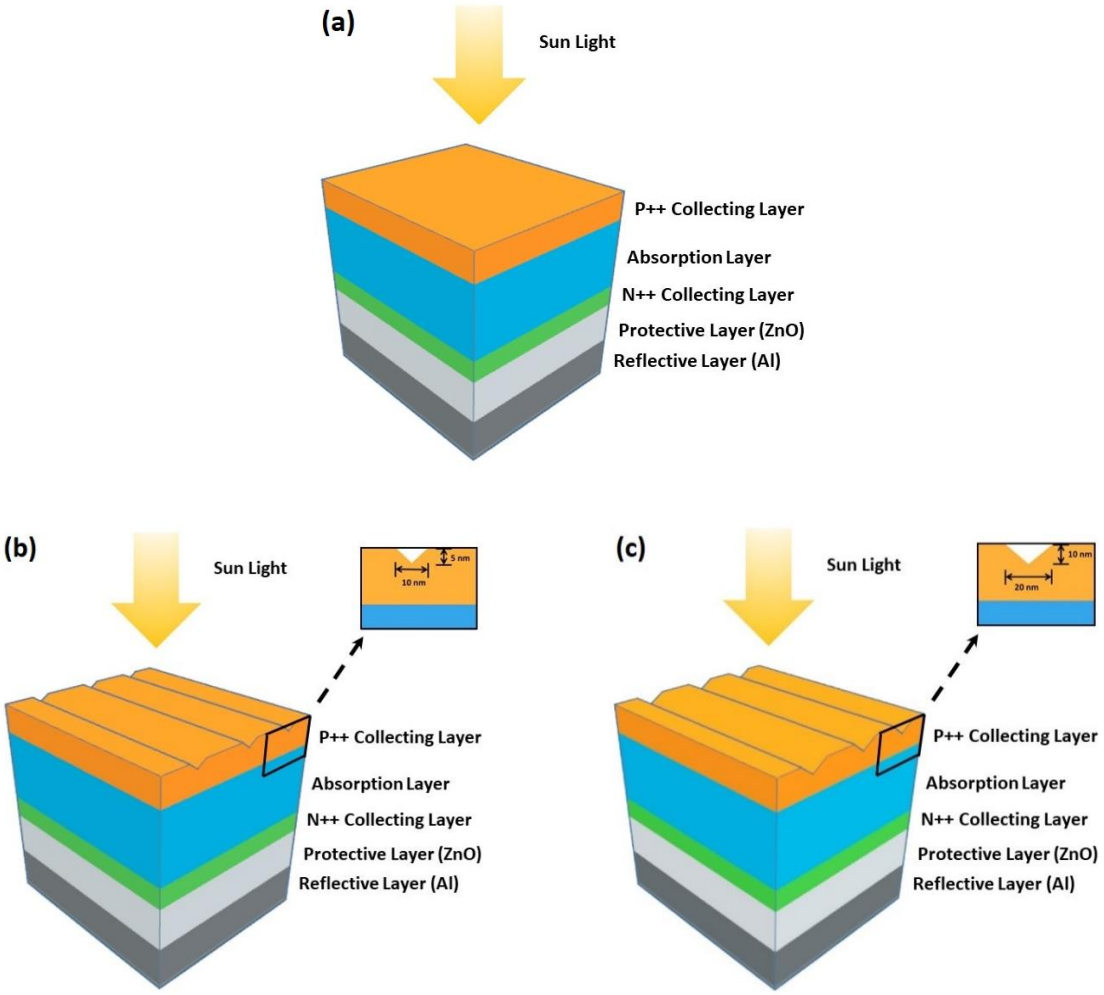

Fig. 1. Structure of the PIN device with different cases of grating.

Table. 1. The values assigned to each parameter in the thin film solar cell

Parameter name	Value
Anode doping concentration (P++-doping)	1e19 (1/cm3)
Cathode doping concentration (N++-doping)	1e19 (1/cm3)
a-Si, intrinsic carrier concentration	1.5e10 (1/cm3)
Thickness (I, Si)	260 nm
Thickness (N++, Si)	40 nm
Thickness (P++, Si)	40 nm
Thickness (ZnO)	75 nm
angle of incidence	[0°]
a-Si, electron mobility	1500 (cm2/(V.s))
a-Si, hole mobility	450 (cm2/(V.s))
Si, band gap @300 K	1.74 [eV]
Si, electron affinity	4.00 [eV]

The doping profile of the PIN layers employed in this work is appeared in Fig. 2. According to the process variation **[17]**, the N++ layer is doped by 1×10^{19} atom/cm^3 and reaches 1×10^{18} atom/cm^3 along the layer thickness, thus we built a very thin doped layer of 20 nm of 1×10^{18} atom/cm^3 (the same has been introduced for P++ layer). The intrinsic layer of 260 nm thickness is used to separate the two doped layers.

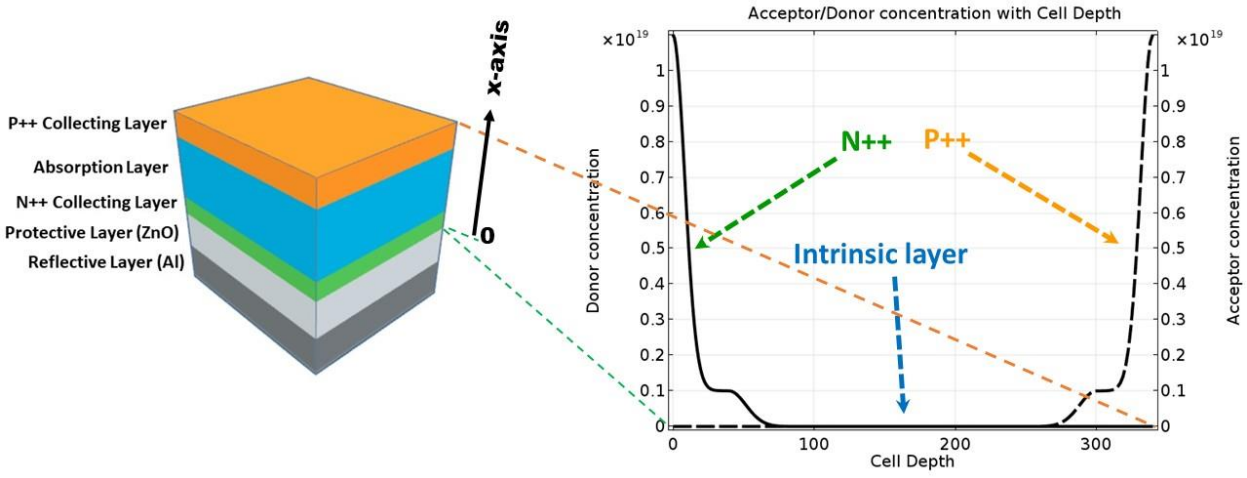

Fig. 2. The doping profile in PIN device model **[18]**.

3. SIMULATION DETAILS AND RESULTS.

3.1. 3D simulation results

In this work, the 3D numerical simulation results of COMSOL Multiphysics **[19]** is used for studying the PV behavior. We integrated the electromagnetic model with the semiconductor model to solve consistently the electrostatics with the optical PV behavior. The structure of thin film solar cell simulation model using the COMSOL MULTIPHYSICS is organized as following:

- Defining the global electrical/optical parameters for the model, e.g., material properties,
- Creating the 3D structure the thin film PV cell,
- Defining the parameters of electromagnetic model such as input/output ports of incident light power.
- Defining the semiconductor parameters such as the position and the dimensions of conducting anode/cathode terminals besides doping profile.
- Selecting the proper mesh shape for solving the differential equations for keeping the solution convergence.
- Defining the electromagnetic-semiconductor output parameters.

In other words, to simulate the proposed structure, initially we must build the structure in 3D domain then applying the electromagnetic model. From Eq. 1 and Eq. 2, if α and $I_f(x, y, z)$ are the absorption coefficient, and the intensity of the photons respectively, then the relationship for the optical absorption for the differential length (D_x, D_y, D_z) is given bellow **[16].**

$$\overrightarrow{I_f}(x,y,z) = I_{f_x}(x,y,z)\hat{x} + I_{f_y}(x,y,z)\hat{y} + I_{f_z}(x,y,z)\hat{z} \quad (1)$$

$$\frac{\partial I_{f_x}(x,y,z)}{\partial x}\hat{x} + \frac{\partial I_{f_y}(x,y,z)}{\partial y}\hat{y} + \frac{\partial I_{f_z}(x,y,z)}{\partial z}\hat{z} = -\alpha\overrightarrow{I_f}(\mathrm{x},\mathrm{y},\mathrm{z}) \quad (2)$$

The solution of Eq. 1, and Eq. 2 are clearly show that the intensity of a photon decreases exponentially with the propagation distance through the semiconductor material due to the absorption **[20-22]**. Meanwhile, the number of electron-hole pairs generated by the light can be expressed as, **[21]**:

$$G(x,y,z) = \frac{\alpha\left(\sqrt{I_{f_x}(x,y,z)^2 + I_{f_y}(x,y,z)^2 + I_{f_z}(x,y,z)^2}\right)}{hf} \quad (3)$$

where h is plank constant, and f is frequency of the wave. Subsequently, to calculate the free electron density and free hole density in semiconductor model, Poisson's Equation is used:

$$\nabla.(\epsilon_r \nabla V) = q(n - p + N_A^- - N_D^+) \quad (4)$$

The carrier transport are governed by continuity equation as following:

$$\frac{1}{q}\nabla.J_n = -U_n \ , \ \frac{1}{q}\nabla.J_p = -U_p$$

where J_n (electron current), J_p (hole current).

Both electron and hole current densities are governed by the hydrodynamic model to account the temperature effects as following

$$J_n = \left(\mu_n \nabla E_c + \frac{qD_{n,th}}{T_1}\nabla T_1\right) n + \mu_n K_B T_1 G(n/N_c)\nabla_n \quad (5)$$

$$J_p = \left(\mu_p \nabla E_v + \frac{qD_{p,th}}{T_1}\nabla T_1\right) p - \mu_p K_B T_1 G(p/N_v)\nabla_p \quad (6)$$

where T is the temperature in kelvin , and D_n electron diffusivity, and D_p hole diffusivity

The energy gap are governed by the conduction band and valence band edges as following

$$E_c = -q(V + \chi) \ , E_v = -q(V + \chi + E_g)$$

To configure the recombination process, the Shockley Read Hall recombination rate **[23, 24]** is applied as following :

$$R_n = \frac{n_p - \gamma_n \gamma_p n_{i,eff}^2}{\tau_p(n+n_1)+\tau_p(p+p_1)} \quad (7)$$

$$, R_n = R_p$$

$$, n_1 = \gamma_n n_{i,eff} \ \exp\left(\frac{\Delta E_t}{K_B T}\right)$$

$$, \ p_1 = \gamma_p n_{i,eff} \ \exp\left(-\frac{\Delta E_t}{K_B T}\right)$$

$$, n_{i,eff} = \sqrt{N_{c0} N_{v0}}.exp\left(-\frac{E_g - \Delta E_g}{2K_B T}\right)$$

$$, \Delta E_t = E_t - E_i$$

Where V (Electric Potential), p (Hole concentration), and n (Electron concentration) are variables, q (Electron charge), ε (Optical property of the material), c (Initial value for carrier concentration), ni (intrinsic concentration), τ_n (Electron life time), τ_p (Hole life time), α (absorption coefficient of material), μ_n (Electron mobility), μ_p (Hole mobility). γ_n and γ_p are the electron and hole degeneracy factors, N_c and N_v are the effective densities of states for the conduction and valence band, E_g is the band gap, ΔE_g the band gap narrowing and E_t is the trap energy level. Energy difference between the defect level and the intrinsic level is ΔE_t.

3.2 3D-Temperature effect on PV of surface grating

To account the temperature effects on the PV electrostatics behaviors model temperature to account the PV crystal temperature changes. In this work we applied different range of temperature values from 300 K to 360 K. Solar cells, like other semiconductor devices are temperature sensitive. As temperature increases as semiconductor's bandgap decreases which producing different mobile carriers' level. In other word, as decreasing the energy band gap as increasing the number of conduction electrons. The bandgap can be reduced by raising the temperature value. photons energy is higher than the energy band gap (E_g) of the semiconductor material, which is absorbed into them and created electron-hole pairing **[25]**. In addition, Equation (8) **[26]** describe this band difference based on temperature dependent division, or

$$E_g(T) = E_g(0) - \frac{\alpha T^2}{(T+\beta)} \tag{8}$$

Here, $E_g(T)$ represents the band gap energy at different temperature values, T and $E_g(0)$ is the band gap of the semiconductor at $T \approx 0K$, α and β are two constants.

The short circuit current density, J_{sc} is defined by Equation (9) which shows that the J_{sc} depends on the solar spectral irradiance and on the initial photon flux, N_{ph}.

$$J_{sc} = q \int_{hv=E_g}^{\infty} \frac{dN_{ph}}{dhv}\, dhv \tag{9}$$

The open circuit voltage, V_{oc} is defined as the maximum available voltage at $J = 0$ and can be expressed as,

$$v_{oc} = \frac{kT}{q} ln\left(\frac{J_{sc}}{J_o} + 1\right) \tag{10}$$

Fig. 3 shows, the energy level diagram of model structure (Fig. 1**c**) at temperature value is 300K, and 330K. We noticed that the band gap energy has been decreased significantly for the PV of 10×10 nm grating at surface where it is constant along the PV thickness which improves the device thermally.

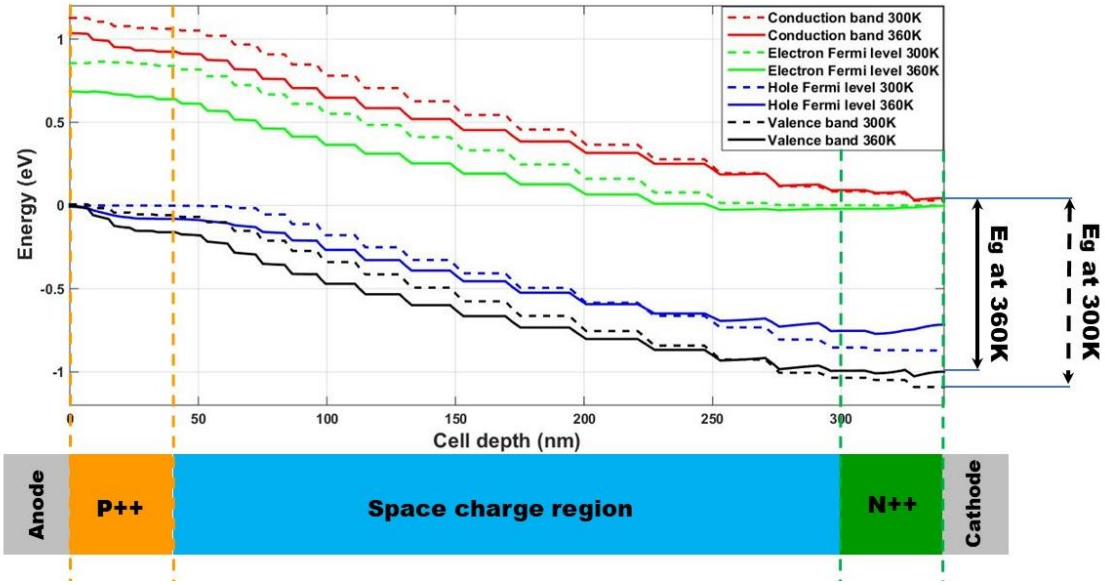

Fig. 3. Energy level diagram for model structure (c) at V_0= 0V.

3.3. Temperature simulation results

The results of the simulation for thin film solar cell model, as shown in Figures 4, 5, 6, 7, 8 and 9 and Table 2, The efficiency of a solar cell has been calculated as a function of temperature. The performance variation in the cell due to varying temperature from 300 to 360 K has been plotted. In figure 4, 5 and 6 the J-V and P-V curves are shown that the all over values are decreases with more temperature in model a and c, but there is no change with model b. Temperature effect on the on the Si thin film solar cell performances (Voc and maximum power of the cell) are showing in figure 7 and 8. A degradation in the open circuit voltage has been achieved of the cell accompany by a degradation in the conversion efficiency and power of the cell. The values of conversion efficiency (η) in figure 9 show that the degradation is approximately liner.

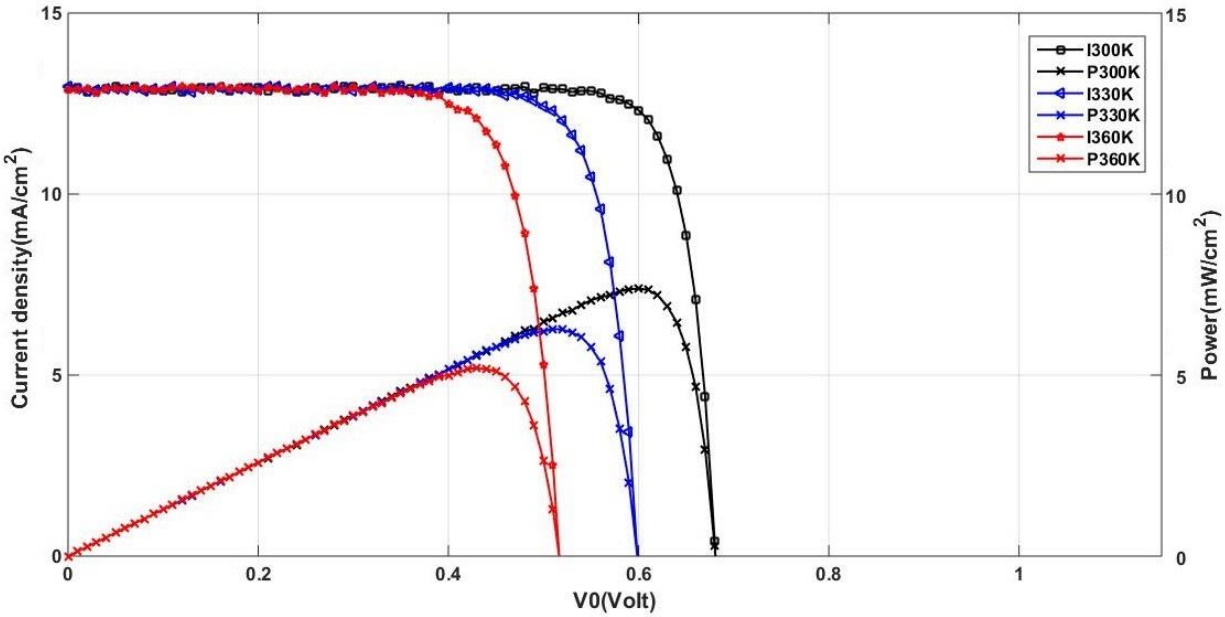

Fig. 4. Temperature dependence of J-V and P-V curves of thin film Solar cell for Model (a) without any grating.

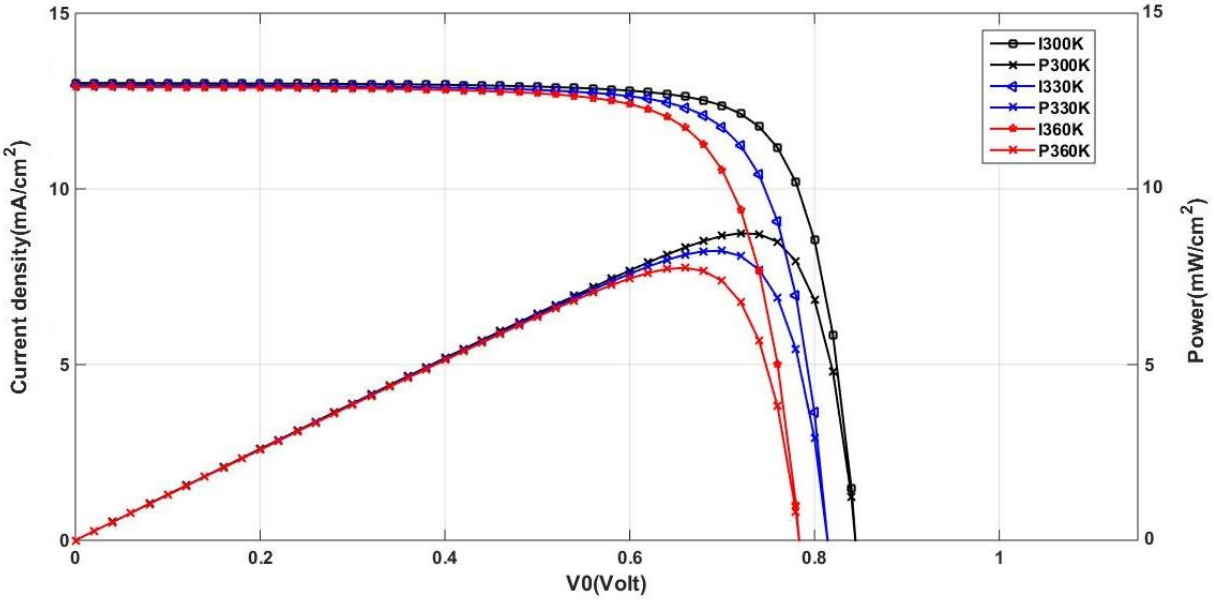

Fig. 5. Temperature dependence of J-V and P-V curves of thin film Solar cell for Model (b) with 5×5 nm grating.

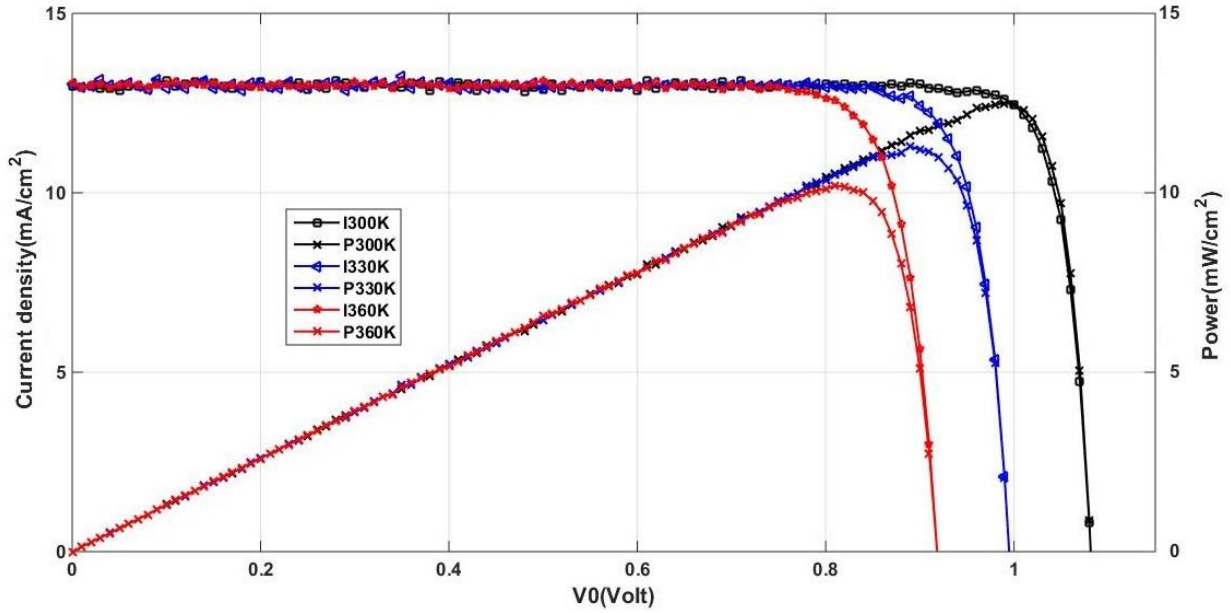

Fig. 6. Temperature dependence of J-V and P-V curves of thin film Solar cell for Model (c) with 10×10 nm grating.

When the temperature increases, the observed diminution in the open circuit voltage (Fig. 4, Fig. 5 and Fig. 6) is due to the increasing in the reverse saturation current density J_0; this increase of J_0 is mainly caused by the increase of the intrinsic carrier concentration n_i and the decreasing in the band gap of the semiconductor material. Also, the increasing of cell temperature affects the material conductivity, which conducts to degradation of the solar cells performances.

Due to the bias of the solar cell junction to the light-generated current, the open-circuit voltage corresponds to the amount of forward bias on the solar cell. Fig. 8 shows the open circuit voltage value of all different models at different temperature levels. The highest conversion efficiency happened at model (Fig. 1c) at 300K of $V_{OC} = 1.08$ V whereas the lowest conversion efficiency at model achieved for device structure of Fig. 1a at 360K of $V_{OC} = 0.51$ V.

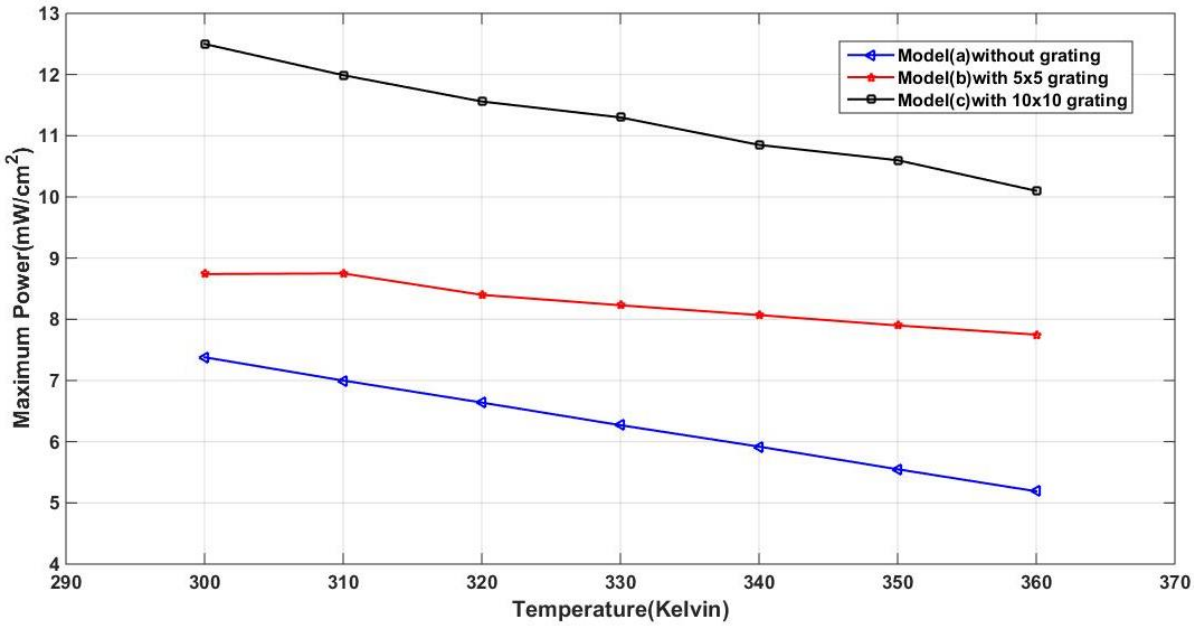

Fig. 7. Maximum power versus temperature.

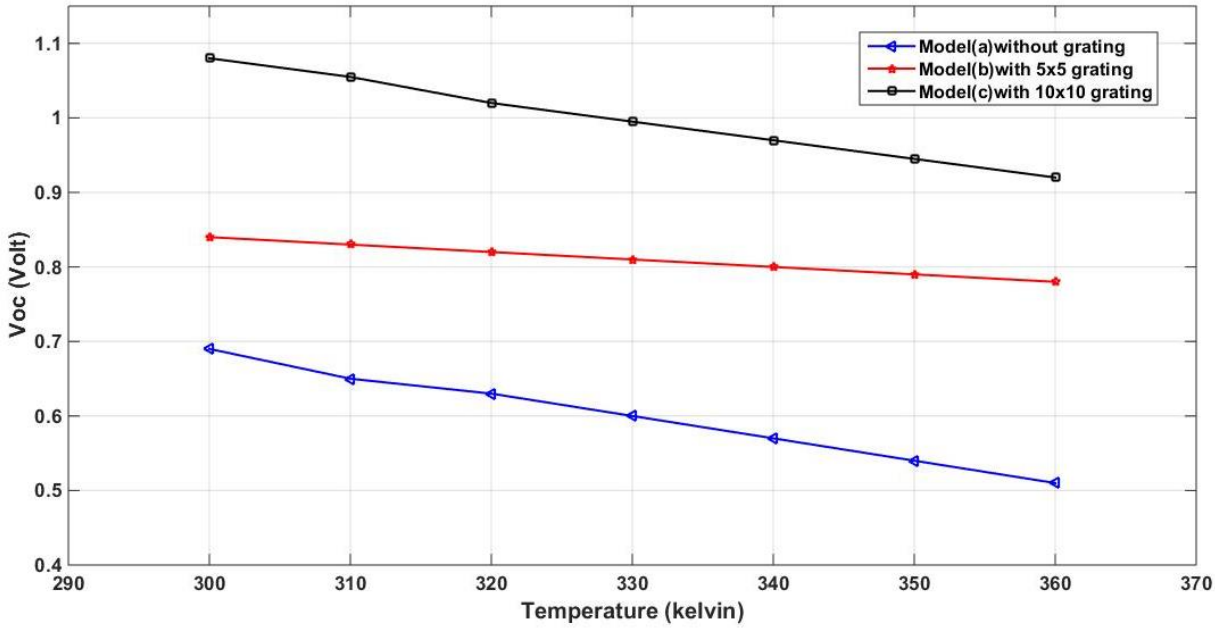

Fig. 8. Open circuit voltage versus temperature.

3.3 Efficiency calculations

Respecting the different PV structures illustrated in Fig. 1, the efficiency has been improved by inserting the surface grating. The efficiency is measured respecting the ratio of energy generated to energy intake from the sun is known as a solar cell's efficiency. The efficiency of a solar cell is determined by the range and strength of incident sunlight, as well as the temperature of the solar cell, in addition to the output of the solar cell. As a result, in order to compare the output of one system to that of another **[16]**.

The fill factor can be calculated as,

$$FF = \frac{I_m V_m}{I_{sc} V_{oc}} \tag{11}$$

The efficiency measurement of a solar cell can be done using Equation (12),

$$\eta = \frac{J_{sc} V_{oc} FF}{P_{in}} \tag{12}$$

Figure 9 indicates that the highest conversion efficiency occurred at 300K of efficiency, η = 12.25 % for PV structure shown in Fig. 1c whereas the lowest conversion efficiency at 360K (η= 5.19 %) for PV structure shown in Fig. 1a.

To study the effect of temperature variance on the thin film solar cell models with different dimensions of triangle grating, Table 2 present the parameters values (P_m, V_{oc}, I_{sc}, P_{max}, I_m, V_m, and η). Table 2 section 1 show model (a) parameters values at different temperature from 300K to 360K minimum efficiency achieved by this model was 5.19% at 360K, and the maximum efficiency due to model a was 7.38%. Table 2 section 2 summarized the value of all parameters for model (b). Finally, in Table 2 section 3 the values of parameters for models (c) the minimum value of efficiency was 10.08% at 360K and the maximum value of efficiency at 300K was 12.25%
.

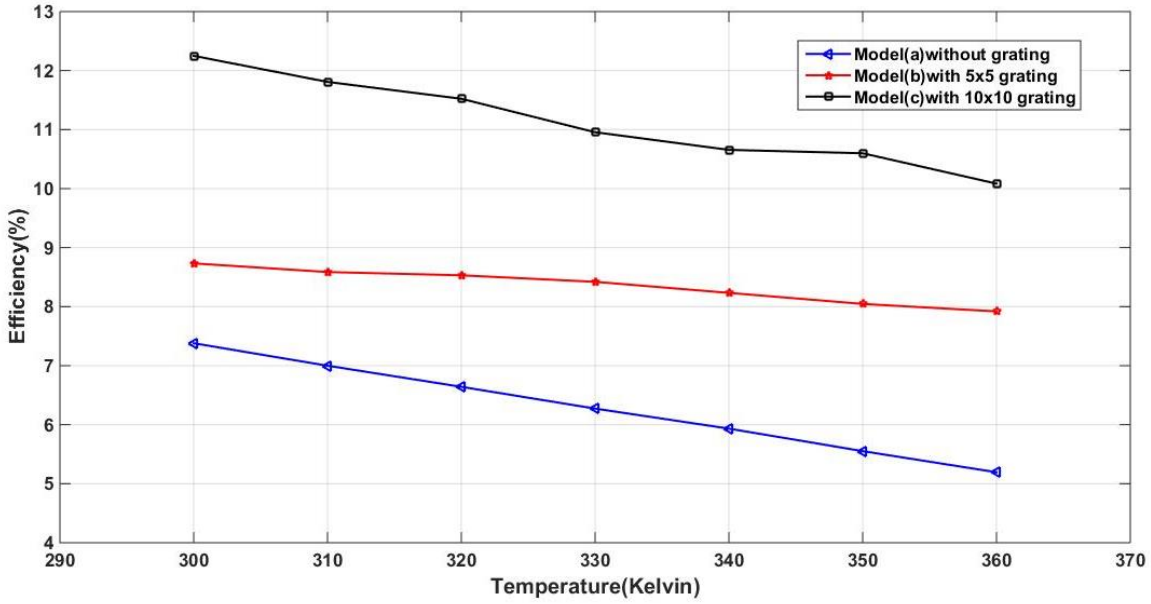

Fig. 9. Efficiency versus temperature.

Table. 2. Models (a), (b), and (c): $P_{in,}$ V_{oc}, P_{max}, J_{sc}, FF, and efficiency at different temperature.

	T(K)	P_{in}(mW/cm^2)	V_{oc}(volt)	J_{sc}(mA)	P_{max}(mw)	J_m(mA)	V_m(Volt)	FF	η(%)
Model (a)	300	100	0.69	13	7.38	12.3	0.6	0.82	7.38
	310	100	0.65	13	7	12.28	0.57	0.83	6.99
	320	100	0.63	13	6.64	12.3	0.54	0.81	6.64
	330	100	0.6	13	6.27	12.3	0.51	0.80	6.27
	340	100	0.57	13	5.92	12.11	0.49	0.80	5.93
	350	100	0.54	13	5.55	12.07	0.46	0.79	5.55
	360	100	0.51	13	5.19	12.08	0.43	0.78	5.19
Model (b)	300	100	0.84	13	8.74	12.13	0.72	0.799	8.733
	310	100	0.83	13	8.75	12.06	0.712	0.795	8.586
	320	100	0.82	13	8.4	12.05	0.708	0.800	8.531
	330	100	0.81	13	8.23	12.03	0.7	0.799	8.421
	340	100	0.8	13	8.07	12.02	0.685	0.791	8.233
	350	100	0.79	13	7.9	12.01	0.67	0.783	8.046
	360	100	0.78	13	7.75	12	0.66	0.781	7.92
Model (c)	300 **[15]**	100	1.08	13	12.5	12.5	0.98	0.87	12.25
	310	100	1.05	13	11.99	12.43	0.95	0.86	11.80
	320	100	1.02	13	11.56	12.39	0.93	0.86	11.52
	330	100	0.99	13	11.3	12.31	0.89	0.84	10.95
	340	100	0.97	13	10.85	12.11	0.88	0.84	10.65
	350	100	0.94	13	10.6	12.47	0.85	0.86	10.59
	360	100	0.92	13	10.1	12.15	0.83	0.84	10.08

From table 2 the temperature degrades PV performance, and this degradation is significantly increased by 4.89 % for the PV without grating compared with the model (b) and model (c)

As shown in up figures the change in the values of the maximum power, open circuit voltage and the conversion efficiency was degraded is approximately liner. The equations (13), (14), and (15) are the result form the model (c) simulation on different temperature.

$$P_{max} = -0.0038T + 24 \quad (13)$$

$$V_{oc} = -0.0028T + 1.9 \quad (14)$$

$$\eta(\%) = -0.035T + 23 \quad (15)$$

4. CAD model for PV with grating

It is necessary to have a model for PV parameters such as short circuit currnet, open circuit voltage, series resistance and shunt resistance to enable the user to simulated the PV within the CAD tools for different applications. Five parameter model the single-diode standard, as shown in the Fig. 10 consist of four main parameters as follows: the existing photovoltaic action source $\boldsymbol{I_{ph}}$, and the diode itself. The ideal recombinant current of electrons and holes in cell-side diffusion and recombination (Shockley diffusion theory), $\boldsymbol{R_{se}}$ and $\boldsymbol{R_{sh}}$ accounting for various causes of loss and no ideals.

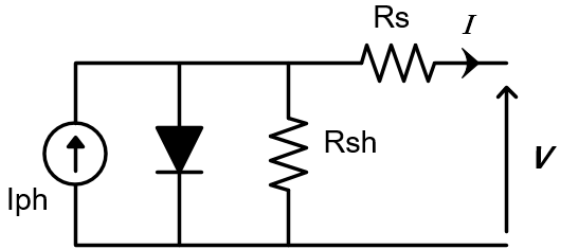

Fig. 10 Equivalent circuit of a solar cell **[27]**.

Where:

$$R_s = \frac{V_{oc} - V_m}{10.I_m} \quad (16)$$

$$R_{sh} = \frac{10.V_m}{I_{sc} - I_m} \quad (17)$$

$$K_1 = \frac{R_{sh} - R_s}{R_s} \cdot \left[\frac{I_m \cdot (R_{sh} + R_s) - V_m}{V_m - I_m \cdot R_s}\right] \quad (18)$$

$$n = \frac{V_m + R_s \cdot (I_m - I_{sc})}{V_t \cdot \ln(K1)} \quad (19)$$

$$I_0 = \frac{R_s \cdot n \cdot V_t}{R_{sh} \cdot (R_{sh} - R_s)} \cdot exp\left[\frac{-I_{sc} \cdot R_s}{n.V_t}\right] \quad (20)$$

$$I_{ph} = I_{sc} + I_0.\left[exp\frac{I_{sc}.R_s}{n.V_t} - 1\right] + \frac{I_{sc}.R_s}{R_{sh}} \quad (21)$$

Where Io is the diode's reverse saturation current, ***n*** is a non-dimensional constant called the ideality factor that defines the diode's deviation from the Shockley diffusion principle, V_{oc} and I_{sc} are respectively the open circuit voltage and the short circuit current **[27]**. Ultimately, the thermal stress is V_t.

Table 3: The values of five parameter model for proposed model (c) from 300K to 360K

	300K	**310K**	**320K**	**330K**	**340K**	**350K**	**360K**
J_{sc} (mA/cm^2)	13	13	13	13	13	13	13
J_m (mA/cm^2)	12.5	12.43	12.39	12.31	12.11	12.47	12.15
V_{oc} (v)	1.08	1.05	1.02	0.99	0.97	0.94	0.92
V_m (v)	0.98	0.95	0.93	0.89	0.88	0.85	0.83
R_s (Ω)	0.8000	0.8045	0.729	0.8123	0.7432	0.7271	0.7407
R_{sh} (kΩ)	19.6	16.67	15.24	12.9	9.89	16.03	9.76
eta	1.0609	1.0487	1.0307	1.0132	1.0330	0.9295	0.9716
J_0 (mA/cm^2)	3.8730e-8	5.290e-8	5.789e-8	8.467e-8	1.401e-7	4.521e-8	1.317e-7
J_{PH} (mA/cm^2)	13	13	13	13	13	13	13

Table 3 present the five model parameters of all proposed model structures in this work. The main value of Table 1 details that we can extract full CAD model for each model structure at different temperature value.

5. CONCLUSIONS

In this paper, both electrical and optical characteristics of the thin film solar cells are examined at the temperature range from 300 K to 360 K. The 3D numerical analysis has been introduced using the COMSOL Multiphysics at which the semiconductor and electromagnetic models are incorporated for studying the electrical and the optical behaviors. The grating generally improved photovoltaic efficiency besides the maximum output power compared to the standard thin film solar cells. A significant improvement is achieved for triangle shaped grating 10×10 nm with based thin film solar cells. A 12.25% of efficiency is obtained from the thin film solar cell with triangle shaped grating 10×10 nm which is higher than the grating free thin film solar cell by 4.87%. Also, we found the triangle shaped grating 10×10 nm provides the maximum efficiency due to all proposed models in all range of temperature variance.

6.

Author Contribution All the authors have contributed equally.

Funding No funding was received.

Data Availability Data related to this article are available from the corresponding author upon reasonable request.

Declarations

Consent to Participate All the authors agreed to involve in this research work.

Consent for Publication All the authors have given permission to publish the results.

Conflict of Interest The authors declare that they have no conflict of interest.

7.REFERENCES

[1]	A.Mc. Evoy, T. Markvart, L. Castaner, Practical Handbook of Photovoltaics Fundamentals and Applications, Second Edition (Elsevier Ltd: 2012).
[2]	L. Zeng et al., "Demonstration of enhanced absorption in thin film Si solar cells with textured photonic crystal back reflector," Appl. Phys. Lett. 93(22), 221105 (2008).
[3]	K. X. Wang et al., "Absorption enhancement in ultrathin crystalline silicon solar cells with antireflection and light-trapping nanocone gratings," Nano Lett. 12(3), 1616–1619 (2012).
[4]	Ahmed E. Khalifa, Hamdy Abd Elhamid, and Mohamed A. Swillam, "Optimal design of intermediate reflector layer in micromorph silicon thin-film solar cells," *Journal of Nanophotonics*, 4(10): 046006-1- 046006-9, 2016.
[5]	G. Landis, R. Rafaelle, D. Merritt, High temperature solar cell development, 19th European Photovoltaic Science and Engineering Conference, Paris, France, June 7–11, 2004.
[6]	J.J. Wysocki, P. Rappaport, Effect of temperature on photovoltaic solar energy conversion, Journal of Applied Physics 31 (1960) 571–578.
[7]	J.C.C. Fan, Theoretical temperature dependence of solar cell parameters, Solar Cells 17 (1986) 309–315.
[8]	P. Singh, S.N. Singh, M. Lal, M. Husain, Temperature dependence of I–V characteristics and performance parameters of silicon solar cell, Solar Energy Materials and Solar Cells 92 (2008) 1611–1616
[9]	D.J. Friedman, Modeling of tandem cell temperature coefficients. in: 25th IEEE Photovoltaic Specialists Conference, Washington DC, IEEE, New York, 1996, pp. 89–92.
[10]	M.A. Contreras, T. Nakada, A.O. Pudov, R. Sites, ZnO/ZnS(O,OH)/Cu(In,Ga)Se2/ Mo solar cell with 18.6% efficiency, in: Proceedings of the Third World Conference of Photovoltaic Energy Conversion, 2003, pp. 570–573
[11]	M.J. Jeng, Yu.L. Lee, L.B. Chang, Temperature dependences of lnxGa1xN multiple quantum well solar cells, Journal of Physics D: Applied Physics 42 (2009) 105101. (pp. 6).
[12]	S.M. Sze, Physics of Semiconductor Devices, John Wiley & Sons, NewYork, 1981, p. 264 (Chapter 14).

[13]	Elewa, S., Yousif, B. & Abo-Elsoud, M.E.A. Efficiency enhancement of intermediate band solar cell using front surface pyramid grating. Opt Quant Electron 53, 360 (2021). https://doi.org/10.1007/s11082-021-03007-6
[14]	Khalil M. ElKhamisy, S. El-Rabaie, Salah S. Elagooz, Hamdy Abd Elhamid" The Effect of Different Surface Grating Shapes on Thin Film Solar Cell Efficiency" International Conference on Innovative Trends in Computer Engineering (ITCE), Aswan, Egypt, 2-4 Feb. 2019.
[15]	Bedir Yousif, Mohy Eldin A. Abo-Elsoud, Hagar Marouf," Triangle grating for enhancement the efciency in thin flm photovoltaic solar cells" Opt Quant Electron **51**, 276 (2019).
[16]	Ahmadreza Ghahremani, and Aly E. Fathy: A three-dimensional multiphysics modeling of thin-film amorphous silicon solar cells. Energy Science and Engineering 3(6), 520–534 (2015). https://doi.org/10.1002/ese3.100
[17]	Marwa Salem, A. Zekry3, and A. Shaker,"Investigation of Base High Doping Impact on the npn Solar Cell Microstructure Performance Using Physically Based Analytical Model"IEEE ACCESS, Vol. 9, pp. 16958-16966,(2021).
[18]	ElKhamisy, K., Abdelhamid, H., Elagooz, S. et al. The effect of different surface plasmon polariton shapes on thin-film solar cell efficiency. Journal of Computational Electronics (2021). https://doi.org/10.1007/s10825-021-01729-0
[19]	Jiazhuang Wang, Zhaopeng Xu, Fei Bian, Haiyan Wang, and Jian Wang "Design and analysis of light trapping in thin-film gallium arsenide solar cells using an efficient hybrid nanostructure," Journal of Nanophotonics 11(4), 046017 (2017). https://doi.org/10.1117/1.JNP.11.046017
[20]	D. Staebler and C. R. Wronski, "Optically induced conductivity changes in dischargeproduced hydrogenated amorphous silicon," J. Appl. Phys. 51(6), 3262–3268 (1980).
[21]	S. Fonash, Ed., "Homojunction solar cells," in Solar Cell Device Physics, pp. 155–166, Elsevier, Burlington, Massachusetts (2012).
[22]	C. Battaglia et al., "Light trapping in solar cells: can periodic beat random?" ACS Nano 6(3), 2790–2797 (2012).
[23]	O. Madelung, "Semiconductors: data handbook," *Springer-Verlag,* Berlin Heidelberg, 2004.
[24]	R. N. Hall, "Electron-hole recombination in silicon," *Phys. Rev.*, 87:387, 1952.
[25]	J. Singh, Electronic and Optoelectronic Properties of Semiconductor Structures, 1 edition. Cambridge; New York: Cambridge University Press, 2007.
[26]	R. Pässler, "Parameter Sets Due to Fittings of the Temperature Dependencies of Fundamental Bandgaps in Semiconductors," phys. stat. sol. (b), vol. 216, no. 2, pp. 975–1007, Dec. 1999.
[27]	Hamdy Abdelhamid, Ahmed Edris, Amr Helmy, and Yehea Ismail," Fast and accurate PV model for SPICE simulation", Journal of Computational Electronics,(18)2,2019,pp. 260-270.